

Designing Gapped Soft Functions for Jet Production

Andre H. Hoang¹ and Iain W. Stewart²

¹*Max-Planck-Institut für Physik (Werner-Heisenberg-Institut)
Föhringer Ring 6, München, Germany, 80805* *

²*Department of Physics, Massachusetts Institute of Technology, Boston, MA 02139* †

Abstract

Distributions in jet production often depend on a soft function, S , which describes hadronic radiation between the jets. Near kinematic thresholds S encodes nonperturbative information, while far from thresholds S can be computed with an operator product expansion (OPE). We design soft functions for jets that serve this dual purpose, reducing to the perturbative result in the OPE region and to a consistent model in the nonperturbative region. We use the $\overline{\text{MS}}$ scheme, and in both regions S displays the appropriate renormalization group scale dependence. We point out that viable soft function models should have a gap associated with the minimum hadronic energy deposit. This gap is connected to the leading $\mathcal{O}(\Lambda_{\text{QCD}})$ renormalon ambiguity in jet event shapes. By defining the gap in a suitable scheme we demonstrate that the leading renormalon can be eliminated. This improves the convergence of perturbative results, and also the stability by which non-perturbative parameters encode the underlying soft physics.

* Electronic address: ahoang@mppmu.mpg.de

† Electronic address: iains@mit.edu

Soft functions play an important role in the study of cross sections close to kinematic thresholds, characterized by jets of collimated hadrons with small invariant mass. These cross sections are frequently described by factorization theorems involving hard Wilson coefficients, jet functions describing the jets of hadrons, and a soft function S . The hard coefficients and the jet functions are perturbative, while S encodes universal nonperturbative information on soft radiation between the jets. The prototype examples are event-shape distributions in e^+e^- annihilation for large c.m. energies Q [1, 2, 3], such as the thrust T [4, 5, 6], where $T \equiv \max_{\hat{n}} \sum_i |\vec{p}_i \cdot \hat{n}| / \sum_i |\vec{p}_i|$ [7] and the kinematically allowed range is $1/2 < T < 1$. In the threshold “dijet” region of large thrust, $T \sim 1$, the events are characterized by two back-to-back jets, and at leading order in $1/Q$ the factorization theorem has two jet functions and one soft function [1, 2, 3]. Other examples include distributions for jet broadening [8], the heavy jet mass [9], and their generalization to angularities [10]. The dijet region also plays a crucial role in event shapes for massive particles, such as the invariant mass distribution of jets from top-quarks [11]. For applications at hadron colliders soft functions which account for initial state radiation are important [12]. Finally, for studies of weak B -meson decays to jets, soft functions involving the initial state B play a crucial role. Examples are $B \rightarrow X_s \gamma$ and $B \rightarrow X_u e \bar{\nu}$ [13, 14, 15], as well as $B \rightarrow X_s \ell^+ \ell^-$ [16, 17]. Here phase space cuts enhance the region where the soft function has a large effect.

Near threshold one can distinguish two regions. Very close to threshold the distribution typically shows an enhanced peaked structure, and nonperturbative information in the soft function is important for determining the shape and the maximum of the distribution. The size of this “peak region” is set by the hadronic scale Λ_{QCD} . Next to the peak region the distribution typically falls off and shows a tail-behavior but is not yet highly suppressed. The dynamics is still dominated by jets and soft radiation, but in this “tail region” the leading soft function can be computed perturbatively since it is probed at scales larger than Λ_{QCD} . In the tail region operators sensitive to nonperturbative physics are power-suppressed. Computations of moments involving integrations over both the peak and tail regions can be done with this same power expansion.

Since S encodes different types of physics in the peak and in the tail region, one possibility is to make separate predictions for the corresponding cross-sections. However, phenomenologically it is often desired to treat both regions coherently. In a pioneering analysis of $e^+e^- \rightarrow \text{jets}$ [18] this was handled by implementing a “hard” IR cutoff on the event shape variable “ e ”. Perturbation theory was used above the cutoff and the perturbative corrections were frozen below it, with

$$R_{\text{PT}}(e, \Lambda_{\text{IR}}) = \theta\left(e - \frac{\Lambda_{\text{IR}}}{Q}\right) R_{\text{PT}}^{\text{NLL}}(e) + \theta\left(\frac{\Lambda_{\text{IR}}}{Q} - e\right) R_{\text{PT}}^{\text{NLL}}(\Lambda_{\text{IR}}/Q), \quad (1)$$

where $R_{\text{PT}}^{\text{NLL}}$ contained perturbative results up to two-loop order with next-to-next-to-leading log resummation (NLL). The function $R_{\text{PT}}(e, \Lambda_{\text{IR}})$ was then convoluted with a normalized soft function model S_{mod} as dictated by the factorization theorem. With a simple choice

for S_{mod} good agreement with LEP data was found for several event shapes. This cutoff procedure does not attempt to treat explicitly the renormalization scale dependence in the region where the soft function is non-perturbative, nor does it systematically implement the perturbative corrections in this peak region.

The multi-region issue has also been analyzed in the context of B -meson decays. In Ref. [19] a perturbative tail was glued to the soft-function model,

$$S(\hat{\omega}, \mu) = S_{\text{mod}}(\hat{\omega}) + \theta(\hat{\omega} - \Lambda - \mu/\sqrt{e})S_{\text{part}}(\hat{\omega}, \mu), \quad (2)$$

where S_{part} is the ‘‘partonic’’ soft function obtained from perturbation theory and where the argument in the θ -function was chosen such that the tail turns on without discontinuity, using the condition $S_{\text{PT}}(\hat{\omega}, \sqrt{e}(\hat{\omega} - \Lambda)) = 0$. This method provides the correct renormalization group behavior for the treatment of the tail region at leading order, and is an improvement because it allows the perturbative jet function corrections to be incorporated systematically in the peak region. Shortfalls are that in the peak region it still hides the dependence on the renormalization scale μ in model parameters, and that the perturbative tail is turned on by hand at a particular point, rather than allowing it to appear once it dominates the non-perturbative corrections.

In this paper we develop a procedure for constructing soft function models for jets that i) reduce to the perturbative result in the OPE region and a consistent model in the nonperturbative region, ii) exhibit the proper renormalization group scale dependence in the $\overline{\text{MS}}$ scheme, iii) have a gap associated with the minimum hadronic energy deposit, and iv) are stabilized to perturbative corrections by being free from the leading $\mathcal{O}(\Lambda_{\text{QCD}})$ renormalon. We show that the soft function gap parameter is essential for removing the renormalon ambiguity of the partonic threshold energy order-by-order in perturbation theory.

Although our procedure is quite general, in order to make all the steps explicit we will carry it out in the context of a specific example. We consider event shapes for top-quark jets produced in $e^+e^- \rightarrow t\bar{t}$ at c.m. energies $Q \gg m_t$. The soft function we construct applies equally well for massless event shapes in the dijet region, that is, very little of our discussion depends on the presence of the top-quark mass or width. We consider the double differential top-antitop invariant mass distribution, $d^2\sigma/dM_t dM_{\bar{t}}$, where $M_{t,\bar{t}}$ are either in the peak or the tail region. In the peak region near the top mass resonance, $s_{t,\bar{t}} \equiv (M_{t,\bar{t}}^2 - m_t^2) \sim m_t\Gamma_t$ where Γ_t is the top-quark width, and we have the factorization theorem [11]

$$\frac{d\sigma^{\text{peak}}}{dM_t^2 dM_{\bar{t}}^2} = \sigma_0 H(Q, m_t, \mu) \int d\ell^+ d\ell^- B_+ \left(\frac{s_t - Q\ell^+}{m_t}, \mu \right) B_- \left(\frac{s_{\bar{t}} - Q\ell^-}{m_t}, \mu \right) S_{\text{np}}(\ell^+, \ell^-, \mu), \quad (3)$$

which is valid at leading order in m_t/Q and Γ_t/m_t . Here H is a calculable hard coefficient and B_{\pm} are calculable jet functions, whereas $S_{\text{np}}(\ell^{\pm}, \mu)$ is a nonperturbative soft function which peaks for $\ell^{\pm} \sim \Lambda_{\text{QCD}}$ when $\mu \sim \ell^{\pm}$. In general the convolution probes momenta

$\ell^\pm \sim s_{t,\bar{t}}/Q$ in the soft function, and large logs in S are avoided by taking $\mu \sim \ell^\pm$ and summing large logs in the jet and hard functions. In the peak region $s_{t,\bar{t}} \sim Q\Lambda_{\text{QCD}} + m_t\Gamma_t$, so the nonperturbative distribution described by $S_{\text{np}}(\ell^\pm, \mu)$ directly effects the differential cross section. On the other hand, in the tail region, $s_{t,\bar{t}} \gg Q\Lambda_{\text{QCD}} + m_t\Gamma_t$, and the dominant momenta in the soft function are $\ell^\pm \sim s_{t,\bar{t}}/Q$. In the interesting region this is a perturbative scale of $\ell^\pm \simeq 3\text{--}30\text{ GeV}$ or larger, depending on the size of Q . The leading order factorization theorem in this tail region is

$$\frac{d\sigma^{\text{tail}}}{dM_t^2 dM_{\bar{t}}^2} = \sigma_0 H(Q, m_t, \mu) \int d\ell^+ d\ell^- B_+ \left(\frac{s_t - Q\ell^+}{m_t}, \mu \right) B_- \left(\frac{s_{\bar{t}} - Q\ell^-}{m_t}, \mu \right) S_{\text{part}}(\ell^+, \ell^-, \mu), \quad (4)$$

which is valid to leading order in $s_{t,\bar{t}}/Q^2$, m_t/Q , and $\Lambda_{\text{QCD}}Q/s_{t,\bar{t}}$. Here the partonic soft function $S_{\text{part}}(\ell^\pm, \mu)$ can be computed as a perturbative series in α_s . Power corrections at $\mathcal{O}(\Lambda_{\text{QCD}}Q/s_{t,\bar{t}})$ are determined from S_{np} in a manner discussed below, while power corrections at $\mathcal{O}(s_{t,\bar{t}}/Q^2)$ involve new factorization theorems containing subleading soft functions (which have been worked out for inclusive B -decays [20, 21, 22, 23]).

The soft function carries information on how soft radiation is associated to the definition of the invariant mass variables $M_{t,\bar{t}}$. To be definite we consider hemisphere mass definitions where the soft function for both Eqs. (3) and (4) is [11]

$$S(\ell^\pm, \mu) \equiv \frac{1}{N_c} \sum_{X_s} \delta(\ell^+ - k_s^{+a}) \delta(\ell^- - k_s^{-b}) \langle 0 | (\bar{Y}_{\bar{n}})^{cd} (Y_n)^{ce} (0) | X_s \rangle \langle X_s | (Y_n)^{ef} (\bar{Y}_{\bar{n}})^{df} (0) | 0 \rangle. \quad (5)$$

Here k_s^{+a} is the total plus-momentum of soft hadrons in X_s that are in hemisphere-a, k_s^{-b} is the total minus momentum for soft hadrons in the other hemisphere. The soft function for thrust is related to the hemisphere soft function by

$$S_T(\tau) = \int d\ell^+ d\ell^- \delta\left(\tau - \frac{\ell^+ + \ell^-}{Q}\right) S(\ell^+, \ell^-), \quad (6)$$

with $\tau \equiv 1 - T$, and we emphasize that $S(\ell^+, \ell^-)$ is independent of the top-mass. In general soft functions are matrix elements of Wilson lines, which in our case are

$$Y_n^\dagger(x) = \text{P exp} \left(ig \int_0^\infty ds n \cdot A_s(ns+x) \right), \quad \bar{Y}_{\bar{n}}^\dagger(x) = \text{P exp} \left(ig \int_0^\infty ds \bar{n} \cdot \bar{A}_s(\bar{n}s+x) \right). \quad (7)$$

In order to predict the invariant mass distribution in the peak and the tail regions we would like to connect Eqs. (3) and (4). In this paper we consider the task of constructing an appropriate soft-function that contains both S_{np} and S_{part} and which can be applied in the peak and the tail region. In order to be useful the result must remain consistent for scales $\mu \sim s_{t,\bar{t}}/Q$, both in the tail region where $s_{t,\bar{t}} \gg Q\Lambda$ and in the peak region where $s_{t,\bar{t}} \sim m_t\Gamma_t + Q\Lambda$. We will consider all large logs to have already been summed by renormalization group evolution from Q down to these μ 's. So the task is to determine the soft function matrix element at these μ 's, where it should contain no large logs.

To begin, consider modeling the soft function by

$$S(\ell^+, \ell^-, \mu) = \int_{-\infty}^{+\infty} d\tilde{\ell}^+ \int_{-\infty}^{+\infty} d\tilde{\ell}^- S_{\text{part}}(\ell^+ - \tilde{\ell}^+, \ell^- - \tilde{\ell}^-, \mu) S_{\text{mod}}(\tilde{\ell}^+, \tilde{\ell}^-), \quad (8)$$

where $S_{\text{part}}(\ell^\pm, \mu)$ is the partonic soft function computed in perturbation theory, and $S_{\text{mod}}(\tilde{\ell}^\pm)$ is a nonperturbative model function that is μ -independent and contributes only for $\tilde{\ell}^\pm \sim \Lambda_{\text{QCD}}$. In Ref. [17] an analog to Eq. (8) was used in the study of $b \rightarrow s\ell^+\ell^-$ to alleviate the issues mentioned about Eq. (2). Taking S_{part} to $\mathcal{O}(\alpha_s)$ this formula provided a simple way of incorporating the cutoff OPE moment constraints of Ref. [19] in the model for the nonperturbative B -meson soft function. Here we will argue that, suitably refined, Eq. (8) can be used to design soft functions for jets that are consistent with the desired properties stated earlier. Defining moments

$$S_{\text{mod}}^{[n,m]} \equiv \int_{-\infty}^{+\infty} d\ell^+ d\ell^- (\ell^+)^n (\ell^-)^m S_{\text{mod}}(\ell^+, \ell^-), \quad (9)$$

we will demand that S_{mod} is normalized, $S_{\text{mod}}^{[0,0]} = 1$. We will also demand that higher moments are finite where we have $S_{\text{mod}}^{[n,m]} \sim (\Lambda_{\text{QCD}})^{n+m}$ for $n + m > 0$.

A virtue of Eq. (8) is that it produces by construction the proper OPE in Eq. (4) when used at a perturbative scale $\mu = \mu_{op} \sim s_{t,\bar{t}}/Q \gg \Lambda_{\text{QCD}}$ where $\ell^\pm \sim s_{t,\bar{t}}/Q$. To see this recall that $\tilde{\ell}^\pm \sim \Lambda_{\text{QCD}}$, and so we can expand S_{part} for $\tilde{\ell}^\pm \ll \ell^\pm$ to give

$$S(\ell^\pm, \mu_{op}) = S_{\text{part}}(\ell^\pm, \mu_{op}) S_{\text{mod}}^{[0,0]} - \left[\frac{d}{d\ell^+} S_{\text{part}}(\ell^\pm, \mu_{op}) S_{\text{mod}}^{[1,0]} + \frac{d}{d\ell^-} S_{\text{part}}(\ell^\pm, \mu_{op}) S_{\text{mod}}^{[0,1]} \right] + \mathcal{O}\left(\frac{Q^2 \Lambda_{\text{QCD}}^2}{s^2}\right). \quad (10)$$

Since $S_{\text{mod}}^{[0,0]} = 1$ we have the desired result that $S(\ell^\pm, \mu_{op}) = S_{\text{part}}(\ell^\pm, \mu_{op})$ at leading power. Computing the renormalized soft function in Eq. (5) to order α_s (Fig. 1 with no n_f -bubbles) it factors as¹

$$S_{\text{part}}^{\text{NLO}}(\ell^\pm, \mu) = S_{\text{part}}^{\text{NLO}}(\ell^+, \mu) S_{\text{part}}^{\text{NLO}}(\ell^-, \mu) \quad (11)$$

with

$$S_{\text{part}}^{\text{NLO}}(\ell, \mu) = \delta(\ell) + \frac{C_F \alpha_s(\mu)}{\pi} \left\{ \frac{\pi^2}{24} \delta(\ell) - \frac{2}{\mu} \left[\frac{\theta(\ell) \ln(\ell/\mu)}{\ell/\mu} \right]_+ \right\}. \quad (12)$$

¹ We note that the factorized form of the soft function with respect to the two hemisphere light-cone variables ℓ^\pm in Eq. (11) allows for the possibility to choose two different μ 's at which to stop running the two jet functions B_\pm in the factorization theorems (3) and (4). While we do not expect that relation (11) is maintained for non-logarithmic corrections beyond the one-loop level, one can prove that the factorized form is maintained to all orders as far the scale-dependence is concerned, as in Eq. (15) [24]. Thus it is possible to treat the situation where s_t and $s_{\bar{t}}$ are widely separated and to account for the resulting non-global logarithms [25] by choosing both renormalization scales differently.

We see explicitly that large logs in $S_{\text{part}}(\ell - \tilde{\ell}, \mu)$ are minimized for $\mu \sim \ell - \tilde{\ell}$. Hence when ℓ and $\tilde{\ell}$ are parametrically different it is the larger of the two that is important for the proper setting of the renormalization scale in the soft function. This is compatible with the expansion in Eq. (10). In the convolution with the jet functions in the tail region in Eq. (4), the logs in S_{part} are minimized for $\mu = \mu_{\text{op}}$, and $S_{\text{part}}(\ell^\pm, \mu_{\text{op}})$ can be determined by a truncated series in $\alpha_s(\mu_{\text{op}})$. Thus for Eq. (4) the result in Eq. (8) works at any order in perturbation theory.

We would also like $S(\ell^\pm, \mu)$ to give a viable model for the peak region $S_{\text{np}}(\ell^\pm, \mu)$ in Eq. (3) when it is applied at a low scale $\mu = \mu_{\text{low}} \gtrsim \Lambda_{\text{QCD}}$. Here $\ell^\pm \sim \tilde{\ell}^\pm$ in $S_{\text{part}}(\ell^\pm - \tilde{\ell}^\pm, \mu)$ for the convolution in Eq. (8). This convolution builds the proper μ -dependence into $S(\ell^\pm, \mu)$, since the μ -dependence is determined by perturbation theory exactly as in $S_{\text{part}}(\ell^\pm, \mu)$. Thus it avoids the issue of having a μ -dependence related to the soft function anomalous dimension in the model parameters in S_{mod} . The convolution with S_{part} also generates a perturbative tail, implying that $S(\ell^\pm, \mu)$ is not normalizable. To see this define the cutoff moments

$$S^{L[n,m]} \equiv \int_{-\infty}^L dl^+ \int_{-\infty}^L dl^- (\ell^+)^n (\ell^-)^m S(\ell^+, \ell^-, \mu). \quad (13)$$

Using Eq. (8) with Eq. (12) and $S_{\text{mod}}^{[0,0]} = 1$ one finds that for $L \gg \Lambda_{\text{QCD}}$ the normalization

$$S^{L[0,0]} = 1 + \frac{C_F \alpha_s(\mu)}{\pi} \left\{ \frac{\pi^2}{12} - 2 \ln^2 \left(\frac{L}{\mu} \right) \right\} + \dots, \quad (14)$$

up to terms of $\mathcal{O}(\alpha_s^2)$ or $\mathcal{O}(\Lambda_{\text{QCD}}/L)$. Rather than a deficiency, this behavior of $S^{L[0,0]}$ is a necessary feature, as it is consistent with the renormalization equations for $S(\ell^\pm, \mu)$. Only S_{mod} needs to be normalized.

For the peak region, perturbative improvements to S_{part} in Eq. (8) that cause a large change to S , could in principle be compensated by changes to the model parameters in S_{mod} . However, it is quite desirable to make S_{part} and S_{mod} as independent as possible, so that the interpretation of the model parameters remains unchanged as we perturbatively improve S_{part} . A measure for this independence is the convergence of the perturbative expansion for S_{part} at μ_{low} . In general the convolution in Eq. (8) generates double logarithmic terms, $\ln^2(\ell/\mu_{\text{low}}) \sim \ln^2(\Lambda_{\text{QCD}}/\mu_{\text{low}})$ in $S(\ell^\pm, \mu_{\text{low}})$ where the scale Λ_{QCD} is set by parameters in S_{mod} . The choice of μ_{low} should be small enough to avoid these potentially large logarithms, but large enough to ensure the validity of the perturbative expansion in $\alpha_s(\mu_{\text{low}})$. Thus a satisfactory choice of μ_{low} might be difficult to find, and requires careful examination. To test this issue we can determine the logarithmic series for $S_{\text{part}}(\ell^\pm, \mu)$, by finding the partonic soft function in renormalization group improved perturbation theory at LL order, NLL order, etc. The renormalization group improved S_{part} satisfies the exact relation

$$S_{\text{part}}(\ell^+, \ell^-, \mu) = \int dl'^+ dl'^- U_s(\ell^+ - \ell'^+, \mu, \mu_0) U_s(\ell^- - \ell'^-, \mu, \mu_0) S_{\text{part}}(\ell'^+, \ell'^-, \mu_0), \quad (15)$$

where U_s is the LL, NLL, etc. evolution kernel. As indicated this kernel factors in the variables ℓ^+ and ℓ^- to any order in perturbation theory [24]. Using this RG-improved $S_{\text{part}}(\ell^\pm, \mu)$ the full $S(\ell^\pm, \mu)$ in Eq. (8) also satisfies the evolution equation (15) exactly, with a μ -independent $S_{\text{mod}}(\tilde{\ell}^\pm)$. When the logs are small we can expand the RG-improved result to a fixed order in $\alpha_s(\mu)$, and the resulting S_{part} and S satisfy the RG to this order. We will use this truncated version of the NLL series for $S_{\text{part}}(\ell^\pm, \mu)$ to test for a choice of μ which minimizes large logs in the soft function. This will also provide a test for the stability of model parameters to the addition of perturbative corrections.

Lets construct the NLL partonic soft function using a Fourier transform as in [26]. At NLL order the partonic soft functions factorize $S_{\text{part}}^{NLL}(\ell^+, \ell^-) = S_{\text{part}}^{NLL}(\ell^+)S_{\text{part}}^{NLL}(\ell^-)$. The Fourier transform of $S_{\text{part}}(\ell) = \int d\ell' U_s(\ell - \ell', \mu, \mu_0)S_{\text{part}}(\ell', \mu_0)$ is a simple product equation

$$\tilde{S}_{\text{part}}(y, \mu) = \tilde{U}_s(y, \mu, \mu_0) \tilde{S}_{\text{part}}(y, \mu_0), \quad (16)$$

where the position space kernel is

$$\tilde{U}(y, \mu, \mu_0) = (i y \mu_0 e^{\gamma_E})^{\omega(\mu, \mu_0)} e^{K(\mu, \mu_0)}. \quad (17)$$

The LL results for ω and K involve Γ_0^{cusp} and β_0 and the NLL results involve Γ_1^{cusp} and β_1 ,

$$\begin{aligned} \omega(\mu, \mu_0) &= \frac{\Gamma_0^{\text{cusp}}}{\beta_0} \left[\ln(r) + \left(\frac{\Gamma_1^{\text{cusp}}}{\Gamma_0^{\text{cusp}}} - \frac{\beta_1}{\beta_0} \right) \frac{\alpha_s(\mu_0)}{4\pi} (r-1) \right], \\ K(\mu, \mu_0) &= \frac{2\pi\Gamma_0^{\text{cusp}}}{\beta_0^2} \left\{ \frac{1}{\alpha_s(\mu)} (r-1-r \ln r) + \left(\frac{\Gamma_1^{\text{cusp}}}{\Gamma_0^{\text{cusp}}} - \frac{\beta_1}{\beta_0} \right) \frac{(1-r+\ln r)}{4\pi} + \frac{\beta_1}{8\pi\beta_0} \ln^2 r \right\}, \end{aligned} \quad (18)$$

which also agrees with Ref. [27]. Here $r = \alpha_s(\mu)/\alpha_s(\mu_0)$, $C_F = 4/3$, $\beta_0 = 11 - 2/3n_f$ and $\beta_1 = 34C_A^2/3 - 10C_A n_f/3 - 2C_F n_f$ for n_f light flavors, and the one and two-loop terms of the cusp-anomalous dimension are $\Gamma_0 = 4C_F$ and $\Gamma_1^{\text{cusp}} = 4C_F[(67/9 - \pi^2/3)C_A - 10n_f/9]$ [28]. To obtain a suitable boundary condition to solve Eq. (16) exactly, we note that the series of $[\theta(\ell) \ln^k(\ell/\mu)/\ell]_+$ plus-functions in $S_{\text{part}}(\ell, \mu)$ become a series of $\ln^k[i y \mu e^{\gamma_E}]$ in $\tilde{S}_{\text{part}}(y, \mu)$. Thus in position space we can take a boundary condition where all the logs are absent. For example, using the LO boundary condition $\tilde{S}_{\text{part}}(y, \mu = -ie^{-\gamma_E}/y) = 1$ in Eq. (16) we obtain $\tilde{S}_{\text{part}}^{NLL}(y, \mu) = \exp[K(\mu, -ie^{-\gamma_E}/y)]$. It is straightforward to verify that this partonic soft function satisfies the evolution equation in Eq. (16). Specifying higher order boundary conditions for \tilde{S}_{part} will then properly specify the subleading non-log terms in the series for \tilde{S}_{part} . For instance, $\tilde{S}_{\text{part}}(y, \mu = -ie^{-\gamma_E}/y) = 1 - \pi C_F \alpha_s(-ie^{-\gamma_E}/y\mu)/8$ fixes the NLO boundary condition of Eq. (12). Thus the general solution to Eq. (15) is

$$S_{\text{part}}(\ell, \mu) = \int \frac{dy}{2\pi} e^{i y \ell} \tilde{S}_{\text{part}}(y, -ie^{-\gamma_E}/y) \exp [K(\mu, -ie^{-\gamma_E}/y)]. \quad (19)$$

This result allows us to determine the LL and NLL series. Order by order in perturbation theory the Fourier transform (FT) can be carried out analytically since

$$\text{FT}[\ln^k(i y \mu e^{\gamma_E})] = \frac{d^k}{d\epsilon^k} \frac{e^{\epsilon\gamma_E}}{\Gamma(1-\epsilon)} \left\{ \delta(\ell) - \frac{\epsilon}{\mu} \left[\frac{\theta(\ell) e^{-\epsilon \ln(\ell/\mu)}}{\ell/\mu} \right]_+ \right\} \Big|_{\epsilon=0}. \quad (20)$$

In addition to the leading logs, this inverse Fourier transform gives contributions to non-log terms from the expansion of $e^{\epsilon\gamma_E}/\Gamma(1-\epsilon)$, which are subleading to the momentum space NLL series. As long as such subleading terms are unambiguously defined order by order and obey the RGE, one is free to include them in the NLL result. For our purposes we define the LL, NLL, etc. results as the resummed series obtained in position space, since it is in this space that the evolution equations are the simplest. With the NLO boundary condition and NLL evolution we find

$$\begin{aligned}
S_{\text{part}}(\ell, \mu) = & \delta(\ell) + \frac{\alpha_s(\mu)C_F}{\pi} \left[-2\mathcal{L}^1 + \frac{\pi^2}{24} \delta(\ell) \right] + \frac{\alpha_s^2(\mu)}{\pi^2} \left[C_F^2 \left\{ 2\mathcal{L}^3 - \frac{3\pi^2}{4} \mathcal{L}^1 + 4\zeta_3 \mathcal{L}^0 - \frac{\pi^4}{80} \delta(\ell) \right\} \right. \\
& \left. + C_F \beta_0 \left\{ \frac{\mathcal{L}^2}{2} - \frac{\pi^2}{48} \mathcal{L}^0 + \frac{\zeta_3}{3} \delta(\ell) \right\} - \Gamma_1^{\text{cusp}} \left\{ \frac{\mathcal{L}^1}{8} - \frac{\pi^2}{96} \delta(\ell) \right\} \right] \\
& + \frac{\alpha_s^3(\mu)}{\pi^3} \left[C_F^3 \left\{ -\mathcal{L}^5 + \frac{17\pi^2}{12} \mathcal{L}^3 - 20\zeta_3 \mathcal{L}^2 + \frac{\pi^4}{24} \mathcal{L}^1 + \left(\frac{17\pi^2 \zeta_3}{6} - 24\zeta_5 \right) \mathcal{L}^0 + \left(\frac{79\pi^6}{20160} - \frac{20\zeta_3^2}{3} \right) \delta(\ell) \right\} \right. \\
& \left. + C_F^2 \beta_0 \left\{ -\frac{5\mathcal{L}^4}{6} + \frac{7\pi^2}{12} \mathcal{L}^2 - \frac{20\zeta_3}{3} \mathcal{L}^1 + \frac{\pi^4}{36} \mathcal{L}^0 + \left(\frac{7\pi^2 \zeta_3}{18} - 4\zeta_5 \right) \delta(\ell) \right\} \right. \\
& \left. + C_F \beta_0^2 \left\{ -\frac{\mathcal{L}^3}{6} + \frac{\pi^2}{48} \mathcal{L}^1 - \frac{\zeta_3}{3} \mathcal{L}^0 + \frac{13\pi^4}{2880} \delta(\ell) \right\} + C_F \Gamma_1^{\text{cusp}} \left\{ \frac{\mathcal{L}^3}{4} - \frac{7\pi^2}{64} \mathcal{L}^1 + \frac{\zeta_3}{2} \mathcal{L}^0 - \frac{\pi^4 \delta(\ell)}{3840} \right\} \right. \\
& \left. + \left(C_F \beta_1 + \frac{1}{2} \beta_0 \Gamma_1^{\text{cusp}} \right) \left\{ \frac{\mathcal{L}^2}{8} - \frac{\pi^2}{48} \mathcal{L}^0 + \frac{\zeta_3}{12} \delta(\ell) \right\} \right] + \mathcal{O}(\alpha_s^4), \tag{21}
\end{aligned}$$

where $\mathcal{L}^j = 1/\mu [\theta(\ell) \ln^j(\ell/\mu) / (\ell/\mu)]_+$. Note that the coefficients for the terms beyond NLL order are incomplete, namely $\alpha_s^2 \mathcal{L}^0$, $\alpha_s^3 \mathcal{L}^{2,1,0}$, and $\alpha_s^{2,3} \delta(\ell)$. We show coefficients for these terms because of our convention of specifying the series in position space and using the full transform to momentum space. To obtain the complete $\alpha_s^2 \mathcal{L}^0$ and $\alpha_s^3 \mathcal{L}^2$ terms we would need to include the non-cusp part of the two-loop anomalous dimension.

Having determined the desired form of S_{part} in Eq. (8) and a means to test for large logs, we now turn to the nonperturbative information in S_{mod} and the overlap with perturbation theory. To satisfy the moment constraints on $S_{\text{mod}}^{[n,m]}$ one can consider a two parameter model with exponential tails [18]

$$f_{\text{exp}}(\tilde{\ell}^+, \tilde{\ell}^-) = \theta(\tilde{\ell}^+) \theta(\tilde{\ell}^-) \frac{\mathcal{N}(a, b)}{\Lambda^2} \left(\frac{\tilde{\ell}^+ \tilde{\ell}^-}{\Lambda^2} \right)^{a-1} \exp \left(\frac{-(\tilde{\ell}^+)^2 - (\tilde{\ell}^-)^2 - 2b\tilde{\ell}^+ \tilde{\ell}^-}{\Lambda^2} \right), \tag{22}$$

where $\mathcal{N}(a, b)$ ensures f_{exp} is normalized to one, and $b \neq 0$ controls the noninclusive correlation between $\tilde{\ell}^+$ and $\tilde{\ell}^-$. Physically the range $-1 < b < 0$ is favored [18]. In the past this and other models used for soft functions in jet physics are taken to be nonzero for $\tilde{\ell}^\pm \geq 0$. This is a natural constraint given that it is satisfied to any order in perturbation theory for $S_{\text{part}}(\tilde{\ell}^\pm)$. With $\tilde{\ell}^\pm \geq 0$, Eq. (8) enforces $\ell^\pm \geq 0$ in $S(\ell^\pm, \mu)$. However, a better approximation is to take a soft-function with a gap so that the soft-function model vanishes for $\tilde{\ell}^\pm < \Delta$,

$$S_{\text{mod}}(\tilde{\ell}^+, \tilde{\ell}^-) = f_{\text{exp}}(\tilde{\ell}^+ - \Delta, \tilde{\ell}^- - \Delta). \tag{23}$$

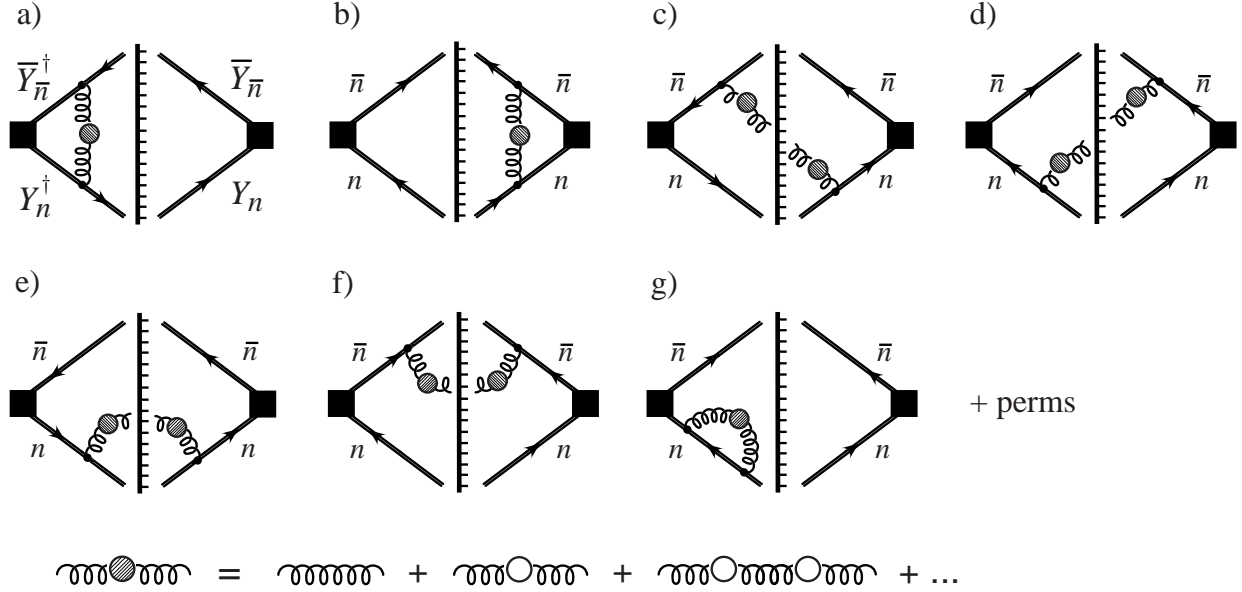


FIG. 1: Graphs for the hemisphere soft function with bubble chains. The solid lines denote Y -Wilson lines, and the line with ticks is the final state cut which may also cut a quark bubble.

Here Δ encodes the minimum hadronic energy deposit in each hemisphere.² Since the model parameter $\Delta \sim \Lambda_{\text{QCD}}$ it has an $\mathcal{O}(1)$ effect in the tail region where the soft function is nonperturbative. Among the model parameters Δ plays a special role because it enables a hadronic interpretation for the variables $\tilde{\ell}^\pm \geq \Delta$ in $S_{\text{mod}}(\tilde{\ell}^\pm)$.

Through the convolution in Eq. (8) this gap is transferred to give $\ell^\pm \geq \Delta$ in $S(\ell^\pm, \mu)$. This transfer relies on the fact that we have a partonic threshold at zero-momentum, i.e. that $S_{\text{part}}(\ell^\pm - \tilde{\ell}^\pm)$ has support only for $\ell^\pm \geq \tilde{\ell}^\pm$. However, this transfer is not entirely straightforward because in perturbation theory the partonic threshold has a renormalon which yields an $\mathcal{O}(\Lambda_{\text{QCD}})$ ambiguity in Δ . In the Borel transform of the hemisphere soft function considered here, this renormalon corresponds to a pole at $u = 1/2$. Since the soft function is universal for massless jets and top quark jets this renormalon is also behind the $u = 1/2$ Borel pole identified by Gardi [29] in an analysis of event-shape distributions in full QCD for massless partons. The nature of this soft function renormalon is similar to the well known $\mathcal{O}(\Lambda_{\text{QCD}})$ renormalon of the heavy quark pole mass definition, but is not equivalent to it; rather it is specific to the soft function for jets. For example, the $u = 1/2$ renormalon pole of the soft function that occurs in inclusive B decays is solely related to the heavy quark pole mass, and is eliminated by switching to a short-distance threshold mass, see for example [19]. For the case of the top jet event shape distribution considered here the pole mass renormalon

² An even more accurate description of the gap would use $\ell^+\ell^- \geq m_{X_{\text{min}}}^2$, but here there is a ℓ^\pm beyond which S_{mod} is exponentially suppressed, so the difference to Eq. (23) is very small.

is contained in the jet functions [11], and is of no concern for the construction of the soft function. Only gluon fields appear in the matrix element defining our S in Eq. (5).

Using standard renormalon calculus either based on gluon propagators dressed with massless fermion bubble chains or on the modified gluon propagator

$$\frac{1}{q^2 + i0} \rightarrow \left(\frac{e^{5/3}}{\mu^2} \right)^{-u} \frac{-1}{(-q^2 - i0)^{1+u}}, \quad (24)$$

the one-gluon exchange graphs in Fig. 1 give the Borel transform

$$B \left[S_{\text{part}}^{\text{tree}}(\ell^+, \ell^-, \mu) \right] \left(u \approx \frac{1}{2} \right) = \frac{8C_F e^{-5/6}}{\pi\beta_0 \left(u - \frac{1}{2} \right)} \mu \left(\delta(\ell^+) \delta'(\ell^-) + \delta'(\ell^+) \delta(\ell^-) \right). \quad (25)$$

This parameterizes the leading $\mathcal{O}(\Lambda_{\text{QCD}})$ renormalon ambiguity of the tree-level soft function, and has the same form as a shift in the zero point of $\delta(\ell^+) \delta(\ell^-)$ expanded to first order. It is also consistent with the result found by Gardi [29] for thrust, accounting for Eq. (6). Equation (25) can be generalized to soft function diagrams with an arbitrary number of gluons with one gluon modified by Eq. (24). Since one can use the soft limit for the modified gluon momentum (compared to the momenta of the unmodified gluons) only diagrams where the dressed gluon is external need to be considered. The computation of the contributions from the dressed gluon then factorizes from the remaining gluons yielding

$$B \left[S_{\text{part}}(\ell^+, \ell^-, \mu) \right] \left(u \approx \frac{1}{2} \right) = \frac{8C_F e^{-5/6}}{\pi\beta_0 \left(u - \frac{1}{2} \right)} \mu \left(\frac{\partial}{\partial \ell^+} + \frac{\partial}{\partial \ell^-} \right) S_{\text{part}}(\ell^+, \ell^-, \mu). \quad (26)$$

This result parameterizes the leading $\mathcal{O}(\Lambda_{\text{QCD}})$ renormalon ambiguity of the soft function at any order. The Borel pole at $u = 1/2$ leads to instabilities in the perturbative predictions as we systematically include perturbative corrections to S_{part} . As we will see below, such instabilities are for example reflected in S becoming negative in certain ranges of ℓ^\pm , or in an instability of the ℓ^\pm values where S is maximal. Physically, this ambiguity ties together the perturbative physics that we aimed to associate with S_{part} and the hadronic information in S_{mod} , and it must be resolved by experimental information.

In order to remove the ambiguity and allow for a stable determination from experimental data we would like to use a renormalon free scheme for the gap. Thus we take $\Delta = \bar{\Delta} + \delta$ where $\bar{\Delta}$ is a renormalon-free model parameter for the hadronic threshold, and $\delta = \delta_1 + \delta_2 + \dots$ has a perturbative expansion which cancels the renormalon ambiguity in S_{part} . Shifting variables to $\bar{\ell}^\pm = \tilde{\ell}^\pm - \delta$ we have

$$\begin{aligned} S(\ell^+, \ell^-, \mu) &= \int_{-\infty}^{+\infty} d\bar{\ell}^+ \int_{-\infty}^{+\infty} d\bar{\ell}^- S_{\text{part}}(\ell^+ - \bar{\ell}^+ - \delta, \ell^- - \bar{\ell}^- - \delta, \mu) S_{\text{mod}}(\bar{\ell}^+ + \delta, \bar{\ell}^- + \delta) \\ &= \int_{-\infty}^{+\infty} d\bar{\ell}^+ \int_{-\infty}^{+\infty} d\bar{\ell}^- S_{\text{part}}(\ell^+ - \bar{\ell}^+ - \delta, \ell^- - \bar{\ell}^- - \delta, \mu) f_{\text{exp}}(\bar{\ell}^+ - \bar{\Delta}, \bar{\ell}^- - \bar{\Delta}). \end{aligned} \quad (27)$$

To cancel the renormalon ambiguity we must expand Eq. (27) in δ simultaneously with our expansion for $S_{\text{part}} = S_{\text{part}}^0 + S_{\text{part}}^1 + \dots$, so that

$$\begin{aligned}
S_{\text{part}}(\ell^\pm - \delta, \mu) &= S_{\text{part}}^0(\ell^\pm, \mu) + \left[S_{\text{part}}^1(\ell^\pm, \mu) - \delta_1 \left(\frac{d}{d\ell^+} + \frac{d}{d\ell^-} \right) S_{\text{part}}^0(\ell^\pm, \mu) \right] \\
&+ \left[S_{\text{part}}^2(\ell^\pm, \mu) - \left(\frac{d}{d\ell^+} + \frac{d}{d\ell^-} \right) \left\{ \delta_2 S_{\text{part}}^0(\ell^\pm, \mu) + \delta_1 S_{\text{part}}^1(\ell^\pm, \mu) \right\} \right. \\
&\left. + \left(\frac{d^2}{d\ell^{+2}} + \frac{d^2}{d\ell^{-2}} + 2 \frac{d^2}{d\ell^+ d\ell^-} \right) \frac{\delta_1^2}{2} S_{\text{part}}^0(\ell^\pm, \mu) \right] + \dots
\end{aligned} \tag{28}$$

Here $\delta_i \sim \mathcal{O}(\alpha_s^i)$ can be defined with any prescription that removes the $\mathcal{O}(\Lambda_{\text{QCD}})$ renormalon ambiguity, and simultaneously this prescription will define a scheme for the hadronic parameter $\bar{\Delta}$. Note that Δ is renormalization group invariant, thus $\bar{\Delta}$ inherits a scale-dependence if δ is not renormalization group invariant. Moreover, we note that quadratic and higher powers of δ_i that appear in Eq. (28) are required to ensure the consistency of the perturbative scheme. The terms linear in δ_i are the ones relevant for removing the leading $\mathcal{O}(\Lambda_{\text{QCD}})$ ambiguity, having the same form as Eq. (26).

In order to motivate a definition for a subtraction scheme associated to δ consider the first moment $S^{L[1,0]}$ from Eq. (13). For now the upper cutoff L is arbitrary. Starting from Eq. (27) we use the OPE as in Eq. (10) and expand to linear order in δ to obtain

$$\begin{aligned}
S^{L[1,0]} &= S_{\text{part}}^{L[1,0]} - [S_{\text{mod}}^{[1,0]}(\bar{\Delta}) + \delta] \int_{-\infty}^L d\ell^+ \int_{-\infty}^L d\ell^- \ell^+ \left[\frac{\partial}{\partial \ell^+} + \frac{\partial}{\partial \ell^-} \right] S_{\text{part}}(\ell^+, \ell^-, \mu) \\
&= S_{\text{part}}^{L[1,0]} - \delta \int_{-\infty}^L d\ell^+ \int_{-\infty}^L d\ell^- \ell^+ \left[\frac{\partial}{\partial \ell^+} + \frac{\partial}{\partial \ell^-} \right] S_{\text{part}}(\ell^+, \ell^-, \mu) + S_{\text{mod}}^{[1,0]}(\bar{\Delta}),
\end{aligned} \tag{29}$$

where in the second line we dropped α_s corrections to the power correction, and here

$$\begin{aligned}
S_{\text{mod}}^{[1,0]}(\bar{\Delta}) &= \int_{-\infty}^{+\infty} d\tilde{\ell}^+ \int_{-\infty}^{+\infty} d\tilde{\ell}^- \tilde{\ell}^+ f_{\text{exp}}(\tilde{\ell}^+ - \bar{\Delta}, \tilde{\ell}^- - \bar{\Delta}) \\
&= \bar{\Delta} + \int_{-\infty}^{+\infty} d\tilde{\ell}^+ \int_{-\infty}^{+\infty} d\tilde{\ell}^- \tilde{\ell}^+ f_{\text{exp}}(\tilde{\ell}^+, \tilde{\ell}^-).
\end{aligned} \tag{30}$$

When S_{part} in the factorization theorem in Eq. (4) is replaced by the full soft function S , the moment $S^{L[1,0]}$ appears in the small ℓ^\pm region, and relates the small momentum contribution in the leading order factorization theorem with the first power correction. From Eq. (26) it is clear that there is a $\mathcal{O}(\Lambda_{\text{QCD}})$ renormalon ambiguity in $S_{\text{part}}^{L[1,0]}$ which should be canceled by the δ -term in Eq. (29). A suitable form for δ to render the leading order factorization theorem and the first power correction renormalon free is

$$\delta = \frac{\int_{-\infty}^L d\ell^+ \int_{-\infty}^L d\ell^- \ell^+ S_{\text{part}}(\ell^+, \ell^-, \mu)}{\int_{-\infty}^L d\ell^+ \int_{-\infty}^L d\ell^- \ell^+ \left[\frac{\partial}{\partial \ell^+} + \frac{\partial}{\partial \ell^-} \right] S_{\text{part}}(\ell^+, \ell^-, \mu)}. \tag{31}$$

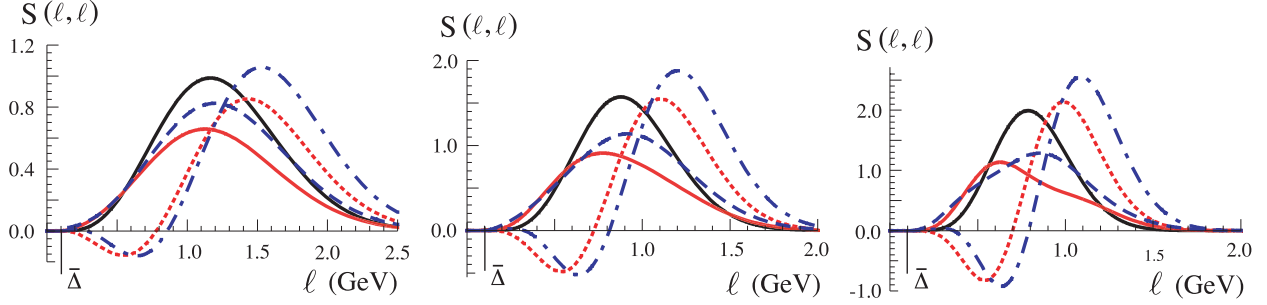


FIG. 2: Soft function $S(\ell^+, \ell^-)$ as a function of $\ell = \ell^+ = \ell^-$ with $\mu = 1$ GeV, at tree level (solid black line), one-loop (dotted red line), one-loop with renormalon subtraction (light solid red line), two-loop NLL (dot-dashed blue line), and two-loop NLL with renormalon subtraction (dashed blue line). Results are shown for three models: $(a, b) = (2.5, -0.8)$ (left panel), $(3.0, -0.5)$ (middle panel) and $(3.5, -0.2)$ (right panel). All models have $\Lambda = 0.55$ GeV and a gap of $\bar{\Delta} = 100$ MeV.

Note that different choices of L correspond to different schemes for renormalon-free gap parameters $\bar{\Delta}$. Other ways to define δ are also feasible. From the expression for S_{part} given in Eq. (21) we obtain

$$\begin{aligned} \delta_1 &= -2L \frac{C_F \alpha_s(\mu)}{\pi} \left[\ln \frac{\mu}{L} + 1 \right], \\ \delta_2 &= -L \frac{\alpha_s^2(\mu)}{\pi^2} \left\{ \beta_0 C_F \left[\frac{1}{2} \ln^2 \frac{\mu}{L} + \ln \frac{\mu}{L} + 1 - \frac{\pi^2}{48} \right] + \Gamma_1^{\text{cusp}} \left[\frac{1}{8} \ln \frac{\mu}{L} + \frac{1}{8} \right] \right. \\ &\quad \left. + C_F^2 \left[\left(\frac{2\pi^2}{3} - 8 \right) \ln \frac{\mu}{L} + 4\zeta(3) + \frac{2\pi^2}{3} - 12 \right] \right\}. \end{aligned} \quad (32)$$

Note that the one-loop δ_1 term is exact, while the two-loop term δ_2 relies on our NLL approximation of Eq. (21).

Lets examine the impact of renormalon subtractions on the soft function. In Fig. 2 $S(\ell^+, \ell^-, \mu)$ is plotted as a function of $\ell = \ell^+ = \ell^-$ at tree-level (solid black line) and one-loop (dotted and lighter solid red lines). Blue dashed and dot-dashed lines are two-loop NLL results to be discussed below. We take $\mu = 1.0$ GeV ($\alpha_s(\mu) = 0.396$) and use the soft model function of Eq. (22) with $\Lambda = 0.55$ GeV, and three different choices $(a, b) = (2.5, -0.8)$ (left panel), $(3.0, -0.5)$ (middle panel), and $(3.5, -0.2)$ (right panel). The dotted red line is the one-loop corrected soft function prior to renormalon subtractions, with $\delta_1 = 0$ and $\bar{\Delta} = \Delta$. The light solid red line is the corresponding result with a renormalon free gap parameter $\bar{\Delta}$, and subtraction using δ_1 from Eq. (32). We use $L = \Lambda$ as a representative scheme choice, and for simplicity have chosen $\bar{\Delta} = 100$ MeV. Other values of $\bar{\Delta}$ simply correspond to a global horizontal shift of all curves by the same amount. While the unsubtracted one-loop soft functions have unphysical negative values for small ℓ , we see that the renormalon-subtracted curves are always positive. This effect of the renormalon subtraction is very general, we have checked that it is realized for any choice of model parameters, renormalization scale μ , and scheme parameter $L \gtrsim \Lambda$. We illustrate this in Fig. 3 by showing soft functions $S(\ell, \ell, \mu)$ with

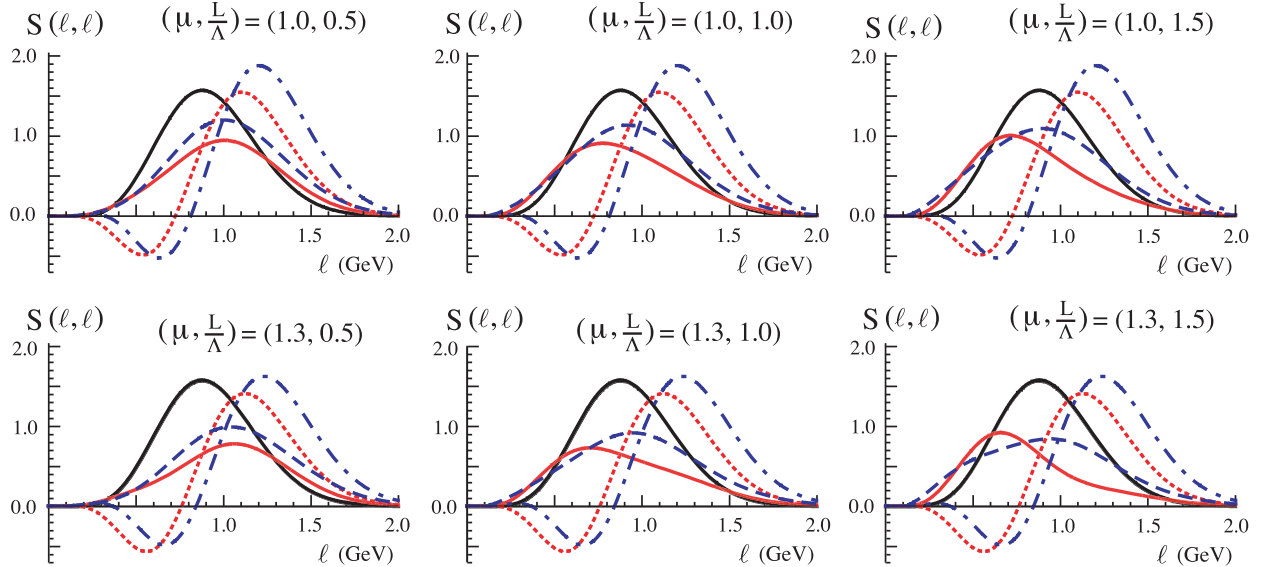


FIG. 3: Dependence of the soft function $S(\ell, \ell, \mu)$ on the renormalization scale μ and the renormalon subtraction scheme-parameter L for the model with $\Lambda = 0.55$ GeV and $(a, b) = (3.0, -0.5)$. Lines use the same conventions as for Fig. 2. As indicated the upper and lower panels represent curves for $\mu = 1.0$ and 1.3 GeV, while the left, middle and right panels refer to $L/\Lambda = 0.5, 1.0$ and 1.5 .

$\Lambda = 0.55$ GeV and $(a, b) = (3, -0.5)$, for different choices of μ and L . For the upper (lower) panels $\mu = 1.0$ (1.3) GeV, and for the left, middle and right panels we have $L/\Lambda = 0.5, 1.0$ and 1.5 . Note that the soft function has an anomalous dimension, see Eq. (15) and (14), so its shape and normalization change when varying μ .

In Fig. 2 the subtracted curves also show a somewhat smaller correction to the ℓ value where their maximum is located than the unsubtracted curves, but this effect is more dependent on the choice of parameters, such as the L value, see Fig. 3. At $\mathcal{O}(\alpha_s)$ the perturbative series for the peak position has not yet approached its asymptotic behavior, but we expect the improvement in convergence for the peak position of the soft function to become more pronounced when higher order perturbative results for the soft function are considered.

To test whether S_{part} suffers from large logs for particular values of μ , the $\mathcal{O}(\alpha_s^2)$ NLL predictions for the soft function from Eq. (21) are shown as the blue dot-dashed and dashed lines in Figs. 2 and 3. The dot-dashed curves do not have renormalon subtractions, and again exhibit negative dips. The dashed curve use our renormalon free $\bar{\Delta}$, with subtractions given by the terms in the last set of square brackets in Eq. (28) and δ_1 and δ_2 from Eq. (32). We see that at this order the renormalon subtractions continue to eliminate the negative dip at small ℓ values. The behavior of the peak location for the two-loop NLL result is in general not dramatically improved, but this is simply because the $\mathcal{O}(\alpha_s^2)$ soft function given in Eq. (21) is based on a logarithmic approximation in a region where the logs are not large, and hence does not contain the large renormalon terms of the full two-loop soft function. Finally, for the lower right panel of Fig. 3, we see an indication for an instability

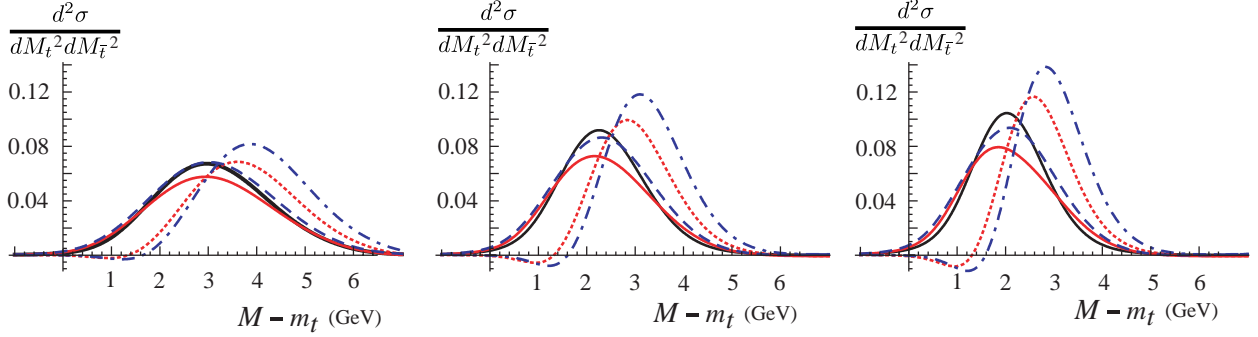


FIG. 4: Top invariant mass distribution $d\sigma/dM_t^2 dM_{\bar{t}}^2$ in the peak region as a function of $M - m_t$ with $M = M_t = M_{\bar{t}}$ accounting only for the perturbative corrections arising from the soft function. The left, middle and right panel refer to the respective models and renormalon subtraction scheme used in Fig. 2 and the same line specifications are employed.

due to increasing logarithmic terms for $\mu = 1.3$ GeV and $L/\Lambda = 1.5$. For the model function of Eq. (22) such regions of instability generally arise for larger values of μ , and increasing positive values of b and L/Λ . This issue might have to be more carefully examined if experimental data suggests that such regions of model parameters are favored.

The impact of the renormalon subtraction is also significant for the differential cross section. Let us first consider the peak region based on the factorization theorem (3). Since we only wish to illustrate the impact of the soft function, we use tree-level jet functions $B_{\pm}(\hat{s}) = 1/(\hat{s}^2 + \Gamma_t^2)$ for $Q/m_t = 5$, $\Gamma_t = 1.43$ GeV, $m_t = 172$ GeV. We also ignore common normalization factors, and evolution factors that sum large logarithms down to the low renormalization scale μ_{low} of the soft function, since they affect all predictions in the same way. (For the case of top-quark jets, a complete analysis including all these terms is carried out in Ref. [24].) Fig. 4 displays this differential cross section for equal invariant masses $M = M_t = M_{\bar{t}}$ over $M - m_t$ for the three parameters sets of Fig. 2. Again we find that using a renormalon free gap parameter improves the convergence of the predictions and avoids the problem of negative dips in the cross-section. Interestingly, the curves show even better convergence compared to the soft function alone, and show nice convergence for the peak location. We find that this is true in general and related to the additional smearing that is provided by the width of the jet function. These results illustrate that the removal of the $\mathcal{O}(\Lambda_{\text{QCD}})$ renormalon contributions in the soft function is essential to obtain a renormalon-free mass measurement from the peak position of the invariant mass distribution. We emphasize again that the renormalon issue in the soft function treated here is entirely independent of the pole mass renormalon problem, which appears in the massive jet function and the top quark pole mass.

Finally, let us examine the tail region of the differential cross section, using again tree-level jet functions and equal invariant masses $M = M_t = M_{\bar{t}}$ and ignoring common normalization factors. To be specific we adopt the model with $\Lambda = 0.55$ GeV and $(a, b) = (3.0, -0.5)$.

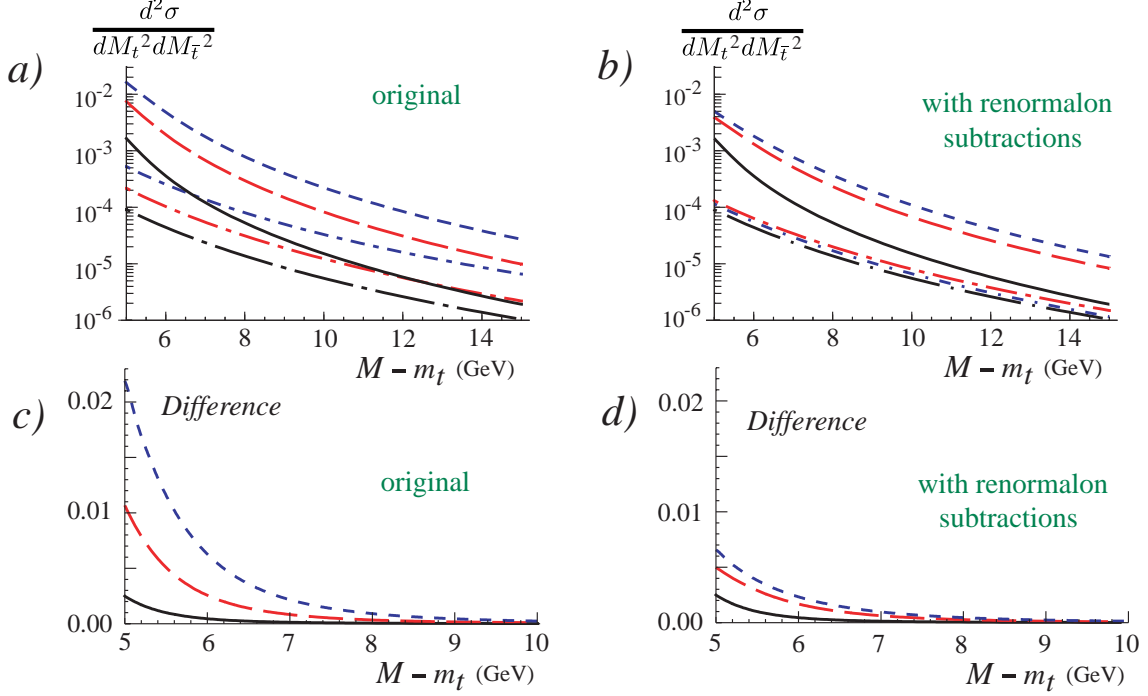


FIG. 5: Top invariant mass distribution $d\sigma/dM_t^2 dM_{\bar{t}}^2$ in the tail region as a function of $M - m_t$, with $M = M_t = M_{\bar{t}}$, $\mu = (M^2 - m_t^2)/Q$, and $\bar{\Delta} = 100 \text{ MeV}$. In a) results are shown without renormalon subtraction ($\delta = 0$), and in b) with a renormalon free gap parameter $\bar{\Delta}$. In a),b) we show: three curves using S_{part} at tree, 1-loop, $\mathcal{O}(\alpha_s^2)$ NLL (long dot-dashed black, medium dot-dashed red, short dot-dashed blue), and three curves using the full S at tree, 1-loop, $\mathcal{O}(\alpha_s^2)$ NLL (solid black, long dashed red, short dashed blue). The latter three curves use the model with $\Lambda = 0.55 \text{ GeV}$ and $(a, b) = (3.0, -0.5)$, and reflect the effects from power corrections when compared to the former three. In c) and d) we show the difference between the first and second set of three curves from a) and b) respectively, at tree (solid black), one-loop (long-dashed red), and $\mathcal{O}(\alpha_s^2)$ NLL (short-dashed blue).

In Fig. 5a the tree-level (black lines), one-loop (red lines) and two-loop (blue lines) cross sections are shown without renormalon subtractions as a function of $M - m_t$. We use $\mu = (M^2 - m_t^2)/Q$ to avoid large logs in the soft function when plotting over a wide range of scales. The dot-dashed lines use the leading order result in Eq. (4) with only the partonic soft function and no gap, and the solid and dashed lines use the full soft function S from Eq. (8) instead and take $\bar{\Delta} = 100 \text{ MeV}$. For a given order in α_s the difference between the curves in Fig. 5a reflect the typical size of power corrections, and are plotted in Fig. 5c. In Fig 5b the same tail distributions as Fig. 5a are displayed, but now with the renormalon subtraction. Since the perturbative contributions in S_{part} are at the scale μ_{op} it is mandatory to choose L of order μ_{op} to avoid large logarithmic terms, as can be also seen from Eq. (31), and we adopt the specific scheme choice $L = \mu_{\text{op}}$. Comparing the curves in Figs. 5a,b we see that the renormalon subtraction substantially improves the perturbative convergence. Figure 5d shows the difference between the solid/dashed and the dot-dashed curves from Fig. 5b.

Comparing it to Fig. 5c we see that the renormalon subtractions lead, as anticipated, to a significantly better perturbative behavior for values one would extract from the data for the power correction.³ This illustrates that the renormalon subtracted predictions are essential for extracting stable and renormalon-free model parameters from experimental data. A scheme such as the one used here, where $L = \mu$, works well for both the tail and peak regions, avoiding large logs. If a result for the gap model parameter is determined from data in a scheme where $L = \mu$, then Eq. (32) can be used to relate the result to other schemes, such as for $L = \mu/2$.

To conclude, we have provided a prescription for designing soft function models in jet production, that can be applied both in the peak region where the soft function is non-perturbative and in the tail region where the soft function can be expanded with an OPE. The method entails the convolution of the partonic soft function with a normalized model function that encodes the nonperturbative information, Eq. (8). It automatically implements consistent renormalization scaling behavior in the $\overline{\text{MS}}$ scheme, making the design particularly useful when dimensional regularization is employed for perturbative calculations. As a novel feature we argue that the soft function models need to exhibit a gap which accounts for the fact that for real hadrons there is a minimal hadronic energy. This gap is also required to devise a systematic scheme to remove the leading $\mathcal{O}(\Lambda_{\text{QCD}})$ renormalon that is contained in the partonic soft function. In Eqs. (27,28, 31) we have provided a simple definition for such a scheme and demonstrated that the removal of the renormalon avoids large uncertainties in predictions of the soft function and hence the cross-section in the peak region. In the tail region it also reduces the size of fluctuations in the power corrections, since they are otherwise affected by the $\mathcal{O}(\Lambda_{\text{QCD}})$ renormalon. It is possible to generalize our method to treat also subleading $\mathcal{O}(\Lambda_{\text{QCD}}^n)$ renormalons with $n > 1$, which are expected to have smaller effect on the soft function stability. Subtraction of these subleading renormalons might improve the numerical stability at higher order in perturbation theory of model parameters in S_{mod} not related to the gap.

Acknowledgments

This work was supported in part by the Department of Energy Office of Nuclear Science under the grant DE-FG02-94ER40818, and in part by the EU network contract MRTN-CT-2006-035482 (FLAVIANet). We thank the Aspen Center for Physics for the inspiring atmosphere provided during the workshop ‘‘Between the LHC and B Factories’’ where the bulk of this work was accomplished. We also thank S. Fleming and S. Mantry for their collaboration on related work [24].

³ Note that our choice of a gap of $\bar{\Delta} = 100$ MeV shifts all curves in Fig. 5a,b that use S to larger values of $M - m_t$. This is a significant power correction, it increases these cross-sections by $\sim 30\%$. However, the choice of $\bar{\Delta}$ does not effect the impact of the renormalon subtraction.

-
- [1] G. P. Korchemsky (1998), hep-ph/9806537, URL <http://arXiv.org/abs/hep-ph/9806537>.
 - [2] G. P. Korchemsky and G. Sterman, Nucl. Phys. **B555**, 335 (1999), hep-ph/9902341, URL <http://arXiv.org/abs/hep-ph/9902341>.
 - [3] C. W. Bauer, C. Lee, A. V. Manohar, and M. B. Wise, Phys. Rev. **D70**, 034014 (2004), hep-ph/0309278, URL <http://arXiv.org/abs/hep-ph/0309278>.
 - [4] S. Catani, G. Turnock, B. R. Webber, and L. Trentadue, Phys. Lett. **B263**, 491 (1991).
 - [5] G. P. Korchemsky and G. Sterman, Nucl. Phys. **B437**, 415 (1995), hep-ph/9411211.
 - [6] Y. L. Dokshitzer and B. R. Webber, Phys. Lett. **B404**, 321 (1997), hep-ph/9704298.
 - [7] E. Farhi, Phys. Rev. Lett. **39**, 1587 (1977).
 - [8] S. Catani, G. Turnock, and B. R. Webber, Phys. Lett. **B295**, 269 (1992).
 - [9] T. Chandramohan and L. Clavelli, Nucl. Phys. **B184**, 365 (1981).
 - [10] C. F. Berger, T. Kucs, and G. Sterman, Int. J. Mod. Phys. **A18**, 4159 (2003), hep-ph/0212343.
 - [11] S. Fleming, A. H. Hoang, S. Mantry, and I. W. Stewart (2007), hep-ph/0703207.
 - [12] N. Kidonakis, G. Oderda, and G. Sterman (1998), hep-ph/9805279.
 - [13] M. Neubert, Phys. Rev. **D49**, 4623 (1994), hep-ph/9312311, URL <http://arXiv.org/abs/hep-ph/9312311>.
 - [14] I. I. Y. Bigi, M. A. Shifman, N. G. Uraltsev, and A. I. Vainshtein, Int. J. Mod. Phys. **A9**, 2467 (1994), hep-ph/9312359, URL <http://arXiv.org/abs/hep-ph/9312359>.
 - [15] T. Mannel and M. Neubert, Phys. Rev. **D50**, 2037 (1994), hep-ph/9402288, URL <http://arXiv.org/abs/hep-ph/9402288>.
 - [16] K. S. M. Lee and I. W. Stewart, Phys. Rev. **D74**, 014005 (2006), hep-ph/0511334, URL <http://arXiv.org/abs/hep-ph/0511334>.
 - [17] K. S. M. Lee, Z. Ligeti, I. W. Stewart, and F. J. Tackmann, Phys. Rev. **D74**, 011501 (2006), hep-ph/0512191.
 - [18] G. P. Korchemsky and S. Tafat, JHEP **10**, 010 (2000), hep-ph/0007005, URL <http://arXiv.org/abs/hep-ph/0007005>.
 - [19] S. W. Bosch, B. O. Lange, M. Neubert, and G. Paz, Nucl. Phys. **B699**, 335 (2004), hep-ph/0402094, URL <http://arXiv.org/abs/hep-ph/0402094>.
 - [20] C. W. Bauer, M. Luke, and T. Mannel, Phys. Lett. **B543**, 261 (2002), hep-ph/0205150.
 - [21] K. S. M. Lee and I. W. Stewart, Nucl. Phys. **B721**, 325 (2005), hep-ph/0409045, URL <http://arXiv.org/abs/hep-ph/0409045>.
 - [22] S. W. Bosch, M. Neubert, and G. Paz, JHEP **11**, 073 (2004), hep-ph/0409115.
 - [23] M. Beneke, F. Campanario, T. Mannel, and B. D. Pecjak, JHEP **06**, 071 (2005), hep-ph/0411395.
 - [24] S. Fleming, A. H. Hoang, S. Mantry, and I. W. Stewart, In preparation (2007).
 - [25] M. Dasgupta and G. P. Salam, Phys. Lett. **B512**, 323 (2001), hep-ph/0104277.
 - [26] G. P. Korchemsky and G. Marchesini, Phys. Lett. **B313**, 433 (1993).
 - [27] M. Neubert (2004), hep-ph/0408179, URL <http://arXiv.org/abs/hep-ph/0408179>.
 - [28] G. P. Korchemsky and A. V. Radyushkin, Nucl. Phys. **B283**, 342 (1987).
 - [29] E. Gardi, JHEP **04**, 030 (2000), hep-ph/0003179.